Diacylglycerol kinase ζ regulates RhoA activation via a kinase-independent scaffolding mechanism

Ryan Ard[a,b], Kirk Mulatz[a,b], Hanan Abramovici[a,b], Jean-Christian Maillet[a,b], Alexandra Fottinger[a,b], Tanya Foley[a,b], Michèle-Renée Byham[a,b], Tasfia Ahmed Iqbal[a,b], Atsuko Yoneda[c], John R. Couchman[c], Robin J. Parks[b,d,e], and Stephen H. Gee[a,b]

[a]Department of Cellular and Molecular Medicine, [b]Centre for Neuromuscular Disease, and [e]Department of Biochemistry, Microbiology and Immunology, University of Ottawa, Ottawa, ON K1H 8M5, Canada; [c]Department of Biomedical Sciences, University of Copenhagen, DK-2200 Copenhagen N, Denmark; [d]Molecular Medicine Program, Ottawa Health Research Institute, Ottawa, ON K1H 8L6, Canada

ABSTRACT **Rho GTPases share a common inhibitor, Rho guanine nucleotide dissociation inhibitor (RhoGDI), which regulates their expression levels, membrane localization, and activation state. The selective dissociation of individual Rho GTPases from RhoGDI ensures appropriate responses to cellular signals, but the underlying mechanisms are unclear. Diacylglycerol kinase ζ (DGKζ), which phosphorylates diacylglycerol to yield phosphatidic acid, selectively dissociates Rac1 by stimulating PAK1-mediated phosphorylation of RhoGDI on Ser-101/174. Similarly, phosphorylation of RhoGDI on Ser-34 by protein kinase Cα (PKCα) selectively releases RhoA. Here we show DGKζ is required for RhoA activation and Ser-34 phosphorylation, which were decreased in DGKζ-deficient fibroblasts and rescued by wild-type DGKζ or a catalytically inactive mutant. DGKζ bound directly to the C-terminus of RhoA and the regulatory arm of RhoGDI and was required for efficient interaction of PKCα and RhoA. DGKζ-null fibroblasts had condensed F-actin bundles and altered focal adhesion distribution, indicative of aberrant RhoA signaling. Two targets of the RhoA effector ROCK showed reduced phosphorylation in DGKζ-null cells. Collectively our findings suggest DGKζ functions as a scaffold to assemble a signaling complex that functions as a RhoA-selective, GDI dissociation factor. As a regulator of Rac1 and RhoA activity, DGKζ is a critical factor linking changes in lipid signaling to actin reorganization.**

Monitoring Editor
Jonathan Chernoff
Fox Chase Cancer Center

Received: Jan 18, 2012
Revised: Aug 3, 2012
Accepted: Aug 14, 2012

INTRODUCTION

Actin cytoskeleton reorganization underlies a variety of cellular activities, including cell migration, cytokinesis, and vesicle trafficking (Etienne-Manneville and Hall, 2002). Rho GTPases are key regulators of actin organization. They function like molecular switches, cycling between inactive, GDP-bound and active, GTP-bound states (Bourne *et al.*, 1990, 1991). In their GTP-loaded conformation they bind downstream effectors to elicit actin reorganization. The activation state of Rho GTPases is tightly controlled by guanine nucleotide exchange factors (GEFs), which activate GTPases by promoting the exchange of GDP for GTP, and by GTPase-activating proteins (GAPs), which inactivate Rho proteins by enhancing their intrinsic GTPase activity (Spiering and Hodgson, 2011). An additional level of regulation is provided by Rho guanine nucleotide dissociation inhibitors (RhoGDIs), which sequester Rho GTPases in inactive cytosolic complexes and prevent their C-terminal isoprenyl group from associating with the plasma membrane where GEFs and effector proteins reside (Dermardirossian and Bokoch, 2005). Furthermore, they protect Rho GTPases from degradation by the proteasome (Boulter *et al.*, 2010).

RhoGDIα is ubiquitously expressed and interacts with at least five different Rho family proteins, including the three best-studied members, RhoA, Rac1, and Cdc42. Each of these mediates the

This article was published online ahead of print in MBoC in Press (http://www.molbiolcell.org/cgi/doi/10.1091/mbc.E12-01-0026) on August 23, 2012.

Address correspondence to: Stephen H. Gee (stevegee@uottawa.ca).

Abbreviations used: BSA, bovine serum albumin; DAG, diacylglycerol; DGK, diacylglycerol kinase; FA, focal adhesion; GAP, GTPase-activating protein; GEF, guanine nucleotide exchange factor; GST, glutathione *S*-transferase; HA, hemagglutinin; HRP, horseradish peroxidase; IB, immunoblot; IP, immunoprecipitation; Kd, kinase-dead; MARCKS, myristoylated alanine-rich C kinase substrate; mDia, mammalian diaphanous 1; MEF, mouse embryonic fibroblast; MLC, myosin light chain; PA, phosphatidic acid; PAK, p21-activated kinase; PDGF, platelet-derived growth factor; PI(4,5)P2, phosphatidylinositol 4,5-bisphosphate; PKC, protein kinase C; PMA, phorbol-12-myristate-13-acetate; RBD, Rho-binding domain; RhoGDI, Rho guanine nucleotide dissociation inhibitor; ROCK, Rho-associated coiled-coil forming protein kinase.

formation of unique actin-based structures. RhoA regulates the assembly of stress fibers and focal adhesions (FAs; Paterson *et al.*, 1990; Ridley *et al.*, 1992), Rac1 regulates lamellipodia formation and membrane ruffling (Ridley *et al.*, 1992), and Cdc42 promotes the extension of filopodia (Nobes and Hall, 1995). To become activated and elicit their biological effects, Rho GTPases must first dissociate from RhoGDI. This occurs in a context-specific manner because upstream signals do not simultaneously activate all Rho proteins. Indeed, recent studies suggest there is precise spatial and temporal regulation of GTPase activation in migrating cells (Spiering and Hodgson, 2011).

There is evidence for a variety of mechanisms to selectively dissociate individual Rho GTPases from RhoGDI, including release by lipids and GEFs and by direct protein interaction (Dermardirossian and Bokoch, 2005). A prominent theme involves direct phosphorylation of RhoGDI by protein kinases, which modulate the affinity for different Rho GTPases (Garcia-Mata *et al.*, 2011). As examples, p21-activated kinase 1 (PAK1) promotes Rac1 release by phosphorylating RhoGDI on Ser-101 and Ser-174 (Dermardirossian *et al.*, 2004), whereas phosphorylation on Ser-34 by protein kinase Cα (PKCα) selectively dissociates RhoA (Dovas *et al.*, 2010). However, evidence from structural studies of RhoGDI in complex with Rho GTPases reveals that key residues making physical contact with RhoGDI are conserved among Rac1, Cdc42, and RhoA (Longenecker *et al.*, 1999; Hoffman *et al.*, 2000; Scheffzek *et al.*, 2000; Grizot *et al.*, 2001). Therefore it has been difficult to reconcile how phosphorylation at specific residues releases some Rho GTPases but not others.

There is growing support for the idea that the required specificity comes from the formation of distinct, multiprotein signaling complexes with individual GTPases. In support of this idea, we recently demonstrated that Rac1 exists in a multiprotein complex with diacylglycerol kinase ζ (DGKζ), syntrophin, PAK1, and RhoGDI (Abramovici *et al.*, 2009). In response to platelet-derived growth factor (PDGF), DGKζ stimulates the production of phosphatidic acid (PA), which induces PAK1 activity. Active PAK phosphorylates RhoGDI and releases Rac1 for activation. Additional evidence comes from a study that showed that fibroblast growth factor 2 binding to syndecan 4 (S4) activates PKCα, which phosphorylates RhoGDI on Ser-96 and triggers the release of RhoG from a complex containing S4 and the scaffold protein synectin (Elfenbein *et al.*, 2009). Such complexes provide a simple and elegant solution for determining the specificity of RhoGDI dissociation.

The release of RhoA involves PKCα-mediated phosphorylation of Ser-34 of RhoGDI (Dovas *et al.*, 2010). Here we demonstrate that DGKζ is a critical component of a complex that includes PKCα, RhoA, and RhoGDI and functions as a RhoGDI dissociation factor specific for RhoA. Our results indicate that optimal RhoA activation and function in mouse embryonic fibroblasts (MEFs) requires DGKζ, but, surprisingly, DGKζ catalytic activity is dispensable, suggesting that it functions primarily as a scaffold. Because DGKζ is common to both Rac1 and RhoA dissociation mechanisms, it might have a role in regulating the balance of Rac1 and RhoA activity.

RESULTS

Decreased RhoA activity in the absence of DGKζ

We previously established that DGKζ-null MEFs have decreased Rac1 activity in comparison with wild-type MEFs but normal Cdc42 activity (Abramovici *et al.*, 2009). To determine whether the absence of DGKζ also causes a change in RhoA activation, we assayed the level of GTP-bound (active) RhoA in lysates of wild-type and DGKζ-null MEFs using a RhoA effector pull-down assay (Ren *et al.*, 1999). There was an approximately threefold decrease in (active) GTP-bound RhoA in resting DGKζ-null cell lysates compared with wild-type lysates (Figure 1, A and B). As expected, there was a substantial increase in RhoA-GTP levels in wild-type cell lysates after serum stimulation. The relative increase in serum-stimulated, null cell lysates was similar (approximately threefold), but the absolute levels were significantly lower than in wild-type cells (Figure 1, A and B). Thus the dramatic decrease in RhoA-GTP levels in the null cells suggests that DGKζ is critical for efficient RhoA activation.

To verify that the decreased RhoA activity is directly due to the loss of DGKζ, we introduced hemagglutinin (HA)-tagged recombinant protein into DGKζ-null cells by adenoviral infection and verified its expression by immunoblotting cell lysates with an anti-DGKζ antibody (Figure 2A). RhoA activity in lysates of cells expressing wild-type HA-DGKζ (AdDGKζ^{wt}) was significantly increased compared to uninfected null cell lysates (Figure 2, A and B). A kinase-dead mutant (AdDGKζ^{kd}) also rescued RhoA activity, suggesting that DGKζ catalytic activity is not necessary for RhoA activation. In contrast, rescue of Rac1 activity in null cells required DGKζ catalytic activity, consistent with our previously published findings (Abramovici *et al.*, 2009). These results argue that the RhoA activation defect in null cells is primarily due to the loss of DGKζ. Moreover, whereas DGKζ enzymatic activity is required for Rac1 activation, it is dispensable for RhoA activation.

DGKζ forms a signaling complex with RhoA and PKCα

A major point of regulation for the Cdc42, Rac1, and RhoA GTPases is their sequestration in an inactive, cytosolic complex by their common inhibitor, RhoGDI (Garcia-Mata *et al.*, 2011). We previously demonstrated that Rac1 is part of a multiprotein signaling complex with DGKζ, syntrophin, PAK1, and RhoGDI (Abramovici *et al.*, 2009). DGKζ-derived PA activates PAK1, which subsequently phosphorylates RhoGDI to trigger Rac1 release. More recently, it was shown that PKCα phosphorylates RhoGDI on Ser-34 to selectively release and activate RhoA (Dovas *et al.*, 2010). Because DGKζ directly interacts with PKCα (Luo *et al.*, 2003a), we hypothesized that it might mediate the formation of an independent signaling complex for RhoA activation.

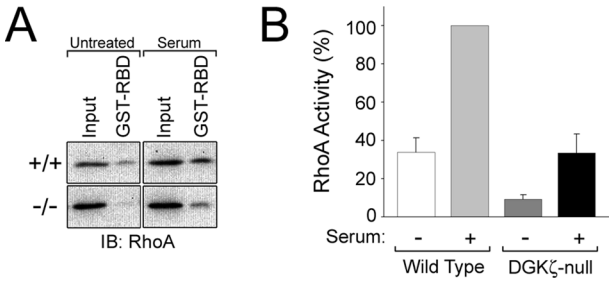

FIGURE 1: Reduced RhoA activity in DGKζ-null fibroblasts (A) Assay of global RhoA GTPase activity. Serum-starved wild-type (+/+) and DGKζ-null (–/–) fibroblasts were treated for 5 min with serum or vehicle alone (untreated). Cell lysates were incubated with an immobilized GST fusion protein of the Rho-binding domain of Rhotekin (GST-RBD) to capture GTP-bound RhoA. The bound proteins were analyzed by immunoblotting (IB) for RhoA. Input represents 10% of the extract used for the pull-down assay (B) Graph showing the quantification of RhoA activity in pull-down assays. The values were normalized to the amount of active RhoA in serum-stimulated, wild-type fibroblasts and are the average of three independent experiments. The errors bars represent SEM.

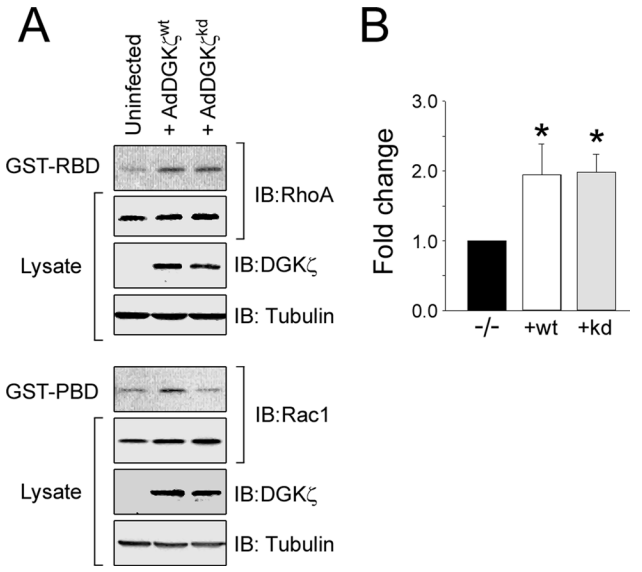

FIGURE 2: Rescue of RhoA activation does not require DGKζ catalytic activity. DGKζ-null fibroblasts were infected with adenovirus bearing HA-tagged, wild-type DGKζ (AdDGKζ^{wt}) or a catalytically inactive (kinase dead) mutant (AdDGKζ^{kd}). RhoA activity was measured as in Figure 1A after serum stimulation of the cells. Global Rac1 GTPase activity was assayed by pull down using immobilized GST fusion protein of p21-binding domain (PBD) of PAK1, followed by immunoblotting for Rac1. The cells were stimulated for 5 min with 50 ng/ml PDGF. The cell lysates were immunoblotted for total RhoA, Rac1, tubulin, and DGKζ. (B) Quantification of active RhoA levels by densitometric analysis of immunoblots. Values are the fold change ± SEM in active RhoA after serum stimulation from three independent experiments. The asterisks indicate a statistically significant difference from null cells ($p < 0.05$) by one-tailed *t* test.

To assess potential interactions between DGKζ and RhoA, we coexpressed epitope-tagged versions of each protein (HA and myc, respectively) in COS-7 cells and subjected them to reciprocal immunoprecipitation and immunoblotting with epitope-tag–specific antibodies. HA-DGKζ was efficiently coprecipitated by anti-myc antibodies when coexpressed with constitutively active myc-RhoA^{V14} or dominant-negative myc-RhoA^{N19} but not when expressed alone (Figure 3A). In the reciprocal experiment, myc-tagged RhoA^{V14} and RhoA^{N19} were effectively coprecipitated by anti-HA antibodies from extracts of cotransfected cells but not from cells expressing HA-DGKζ alone (Figure 3B). No proteins were precipitated by control mouse immunoglobulin G (IgG). Endogenous RhoA was also coimmunoprecipitated with HA-DGKζ from transfected wild-type MEFs (Figure 3C). Moreover, endogenous DGKζ was coimmunoprecipitated by a RhoA antibody, but not by control IgG, from detergent extracts of mouse brain, a rich source of DGKζ protein (Figure 3D). Collectively these results demonstrate that DGKζ forms a stable complex with RhoA under a variety of in vitro, and presumably also in situ, conditions.

Consistent with the idea that DGKζ mediates the interaction of PKCα with RhoA, RhoA was efficiently coimmunoprecipitated with PKCα from wild-type fibroblast extracts but much less so from extracts of DGKζ-null fibroblasts (Figure 3E). Quantification of replicate blots showed a ~2.5-fold decrease in the amount of coprecipitated RhoA from DGKζ-null cells compared with wild-type cells. These data suggest DGKζ is required to efficiently assemble PKCα and RhoA into a signaling complex. RhoGDI was present in PKCα immunoprecipitates from both wild-type and null cell lysates, suggesting that its interaction with PKCα does not depend on DGKζ. As expected, neither Rac1 nor PAK1 coimmunoprecipitated with PKCα, confirming that they are not part of the same signaling complex. Finally, both glutathione *S*-transferase (GST)–RhoA^{V14} and GST-RhoA^{N19} captured myc–α-syntrophin from extracts of transfected wild-type, but not DGKζ-null, MEFs (Figure 3F), suggesting that DGKζ is required for syntrophin to associate with RhoA. Taken together, these results suggest DGKζ is a central organizer of a signaling complex that includes RhoA, PKCα, RhoGDI, and syntrophin.

Direct interaction of DGKζ with RhoA

The results described so far do not exclude the possibility that an additional protein mediates the interaction between DGKζ and RhoA. To determine whether the interaction is direct and to identify the interacting regions, we used a soluble hexahistidine (His_6) fusion protein of RhoA (containing an S-Tag epitope) to overlay various GST fusion proteins of DGKζ, shown schematically in Figure 4A. RhoA consistently bound to a DGKζ fusion protein containing amino acids 97–233, which includes two cysteine-rich regions homologous to the C1A and C1B motifs of PKCs (Figure 4B; Hurley *et al.*, 1997). Of interest, this is the same region that we defined previously as the binding site for Rac1 (Yakubchyk *et al.*, 2005). RhoA did not bind to GST or other GST-DGKζ domains, demonstrating the specificity of the interaction. Additional overlay experiments narrowed down the RhoA-binding site to the C1A domain of DGKζ (Figure 4D). Moreover, both Rac1 and RhoGDI also bound to the same region of DGKζ. We verified that S-protein–horseradish peroxidase (HRP), the reagent used to detect the S-Tag epitope, did not bind to any of the fusion proteins on its own (Supplemental Figure S1). GST-RhoA^{V14} and GST-RhoA^{N19} fusion proteins efficiently captured HA-tagged, wild-type DGKζ from lysates of transfected MEFs but failed to capture a mutant missing amino acids 97–233 (HA-DGKζΔ$^{97–233}$) suggesting that these residues are required for RhoA binding (Figure 4C). Moreover, this region was necessary to rescue RhoA activation in DGKζ-null cells (Figure 4E). In control experiments, HA-DGKζΔ$^{97–233}$ was efficiently captured by the PDZ domain of α-syntrophin, indicating that the deletion does not affect DGKζ function in this regard (Supplemental Figure S2).

Pull-down experiments were used to identify the DGKζ-binding site on RhoA. The C-terminal half of RhoA (amino acids 101–193), but not the N-terminal half (amino acids 1–100) or GST alone, was sufficient to capture HA-tagged DGKζ from transfected fibroblast cell lysates (Figure 4F). Further refinement showed that a fragment containing the last 43 amino acids of RhoA (151–193) was sufficient to bind DGKζ (Figure 4G). The same region of Rac1 was also sufficient to bind DGKζ (Supplemental Figure S3). Collectively these results show the C-termini of RhoA and Rac1 interact directly with the C1A region of DGKζ.

DGKζ binds to the regulatory region of RhoGDI

RhoGDIα is composed of two structurally distinct regions: an N-terminal regulatory domain (residues 1–67) and a C-terminal immunoglobulin-like domain (residues 68–204; Figure 5A). The serine residue (Ser-34) phosphorylated by PKCα lies adjacent to the αB helix within the regulatory arm of RhoGDI. Using pull-down assays, we narrowed down the DGKζ-binding region of RhoGDI to the N-terminal regulatory domain (Figure 5B). A GST fusion protein comprising amino acids 1–67 was sufficient to capture HA-tagged DGKζ from transfected cell lysates, whereas a fusion protein containing amino acids 68–204 failed to capture DGKζ (Figure 5B). Smaller GST fusion proteins (residues 1–33 and 34–67) were not sufficient to

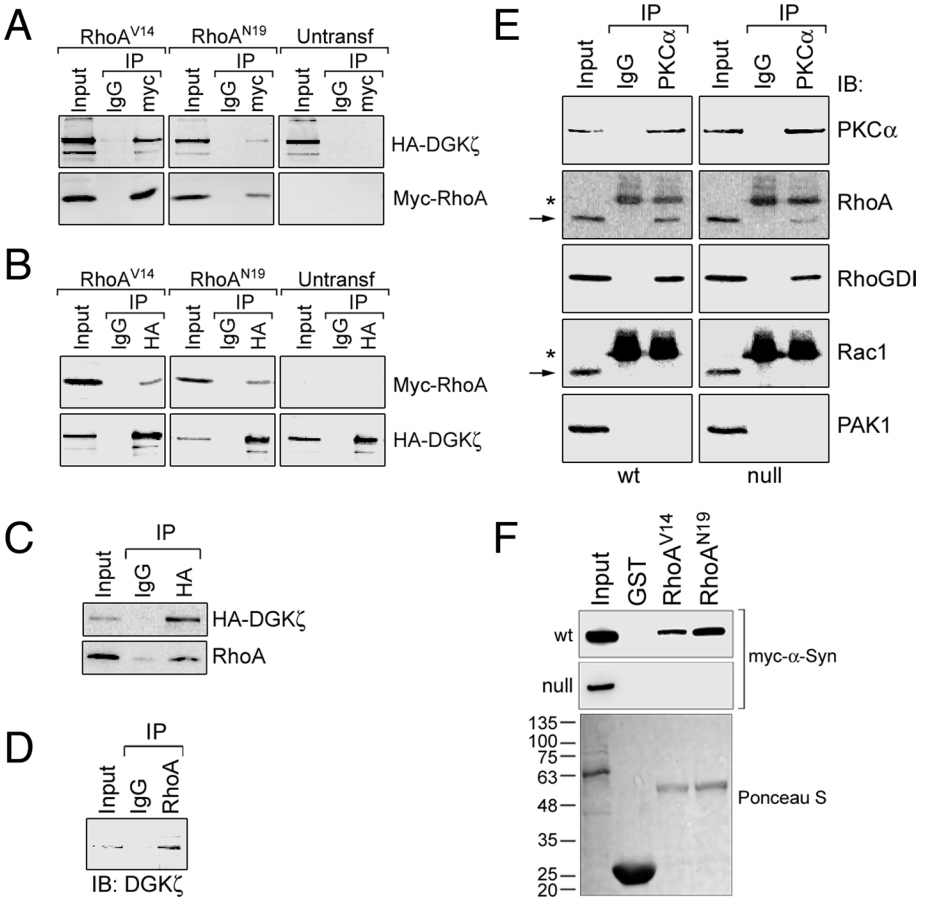

FIGURE 3: DGKζ mediates the formation of stable, multiprotein complex with RhoA, PKCα, syntrophin, and RhoGDI. (A) DGKζ coimmunoprecipitates with constitutively active RhoA^{V14} and dominant-negative RhoA^{N19}. Cos-7 cells infected with an adenoviral construct encoding HA-DGKζ were left untreated or were transfected with myc-RhoA^{V14} or -RhoA^{N19} and allowed to recover for 24 h. Cell extracts were immunoprecipitated (IP) with control IgG or anti-myc antibody. The immune complexes were analyzed by Western blotting with an anti-HA antibody (top). The expression and IP efficiency of the RhoA^{V14} and RhoA^{N19} mutants were monitored by Western blotting of the cell lysates and the IPs, respectively, with anti-myc (bottom). (B) In the reverse experiment, RhoA was detected in HA but not control IgG complexes. No myc-reactive bands were detected in untransfected cells. (C) Lysates of wild-type MEFs infected with HA-tagged DGKζ were subjected to immunoprecipitation with control IgG or an anti-HA antibody. Bound RhoA was detected by immunoblotting. (D) Interaction of endogenous DGKζ and RhoA in rat brain. Detergent extracts of mouse brain were immunoprecipitated with control IgG or an anti-RhoA antibody. The bound proteins were immunoblotted with an anti-DGKζ antibody. (E) Wild-type and DGKζ-null cell extracts were subjected to IP by either control IgG or anti-PKCα antibodies. The immune complexes were analyzed by immunoblotting for PKCα, RhoA, RhoGDI, Rac1, or PAK1. The arrows denote the position of Rac1 and RhoA, whereas asterisks indicate IgG light chains. (F) DGKζ mediates the interaction of RhoA with syntrophin. Lysates of wild-type and DGKζ-null MEFs transfected with myc-α-syntrophin were incubated with GST-RhoA^{V14} or GST-RhoA^{N19}. The bound proteins were analyzed by immunoblotting with an anti-myc antibody.

bind DGKζ. However, in the context of the full-length protein, residues 1–33 were dispensable for binding, whereas 34–58 were essential (Figure 5C). Taken together, these results suggest DGKζ binds to the region of RhoGDI immediately C-terminal to Ser-34.

Reduced Ser-34 phosphorylation of RhoGDI by PKCα in the absence of DGKζ

To determine whether DGKζ is required for PKCα-mediated phosphorylation of Ser-34, we stimulated wild-type and DGKζ-null cells with phorbol-12-myristate-13-acetate (PMA), a potent PKC activator. Immunoblot analysis of the cell lysates was carried out using an affinity-purified antibody that specifically recognizes Ser-34–phosphorylated RhoGDI (Dovas *et al.*, 2010). A faint band corresponding to the size of RhoGDI (~28 kDa) was detected in lysates of untreated wild-type cells (Figure 6A). There was a dramatic increase in intensity of the band after 10 min of PMA stimulation and a further increase at 20 min. The increase was blocked by the specific PKCαβ inhibitor Gö6976. In contrast, PMA stimulation of DGKζ-null cells elicited a much smaller increase in phosphorylated Ser-34. Quantification of signal intensities at the 20-min time point showed a significant decrease ($p < 0.001$) in pSer-34 levels in DGKζ-null cells compared with wild-type cells (Figure 6B). Similar results were obtained using serum-stimulated wild-type and null cells (Supplemental Figure S4, A and B). These data suggest PKCα-mediated phosphorylation of Ser-34 is defective in DGKζ-null cells.

Exogenous expression of HA-tagged DGKζ in PMA-stimulated null cells was sufficient to restore pSer-34 RhoGDI to the level seen in wild-type MEFs (Figure 6C). The kinase-dead DGKζ mutant (DGKζ^{kd}) also rescued the phosphorylation defect, indicating that catalytic activity is dispensable for its role in this complex. Collectively these results indicate that DGKζ is required for optimal Ser-34 phosphorylation by PKCα.

A previous study showed that a phosphorylation-mimicking (S34D) mutation in RhoGDI significantly reduced binding to RhoA, whereas a phosphorylation-deficient (S34A) mutation had little effect (Dovas *et al.*, 2010). Here we compared the ability of the same S34D and S34A mutants to bind DGKζ; however, we observed no significant differences from wild-type RhoGDI (Supplemental Figure S5, A and B**).**

Aberrant stress fiber and focal adhesion formation in DGKζ-null cells

Stress fibers confer contractility on adherent cells and are stimulated by the RhoA signaling pathway (Amano *et al.*, 2010). To determine whether the absence of DGKζ and the resultant decrease in RhoA activity affect stress fiber formation, we stained wild-type and DGKζ-null MEFs spreading on fibronectin with phalloidin to visualize F-actin. Wild-type MEFs had regularly distributed stress fibers that often spanned the length of the cell (Figure 7A). In contrast, stress fibers in DGKζ-null fibroblasts were thicker and appeared less well organized, often radiating from one or more regions of the cell and forming condensed F-actin structures (Figure 7A, arrow). Quantification revealed that these structures were much less frequent in wild-type cells (Figure 7B). To verify that DGKζ loss is the direct cause of the aberrant

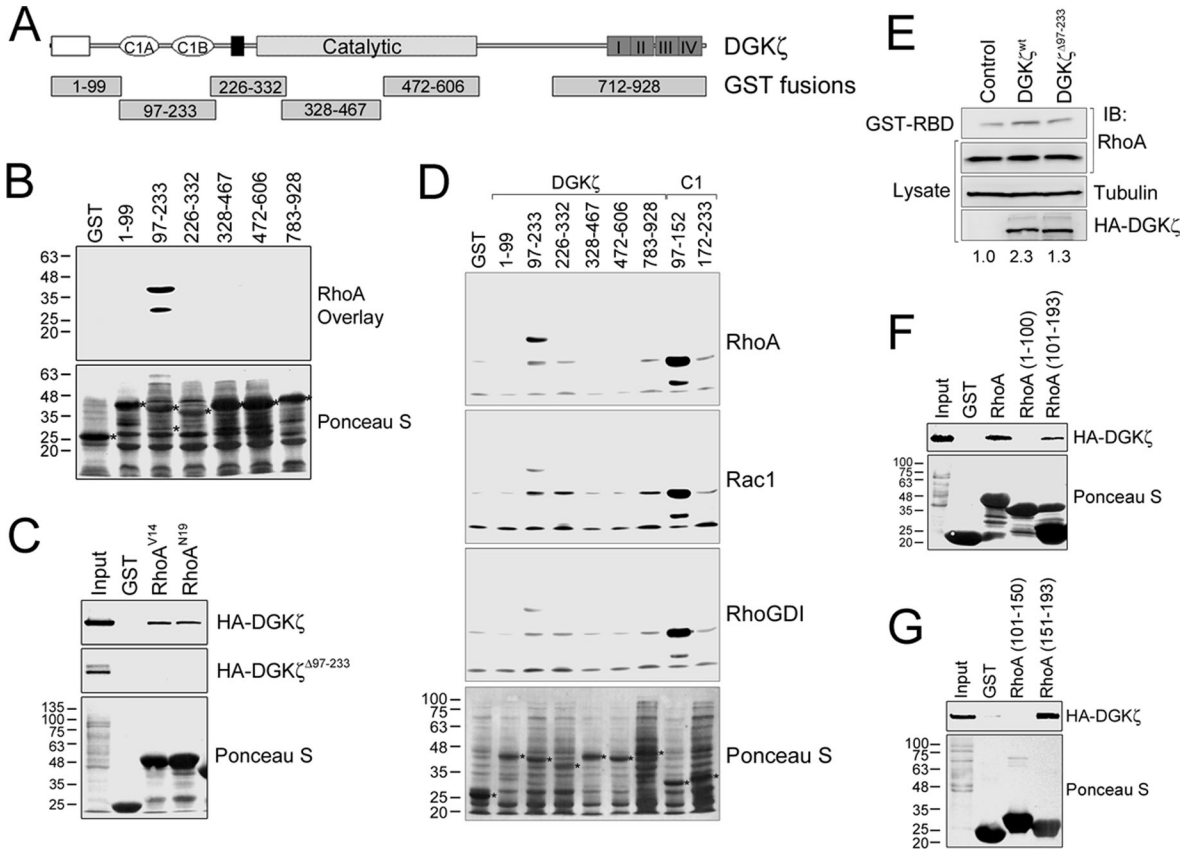

FIGURE 4: Direct interaction of RhoA with DGKζ C1 domains. (A) Schematic showing the domain organization of DGKζ. The N-terminus (open box), C1 (ellipses), MARCKS (filled box), and catalytic domains are indicated. Also shown are the four ankyrin repeats (I–IV) at the C-terminus. Shown below are the amino acid boundaries of the DGKζ constructs that were fused to the C-terminus of GST. (B) The constructs shown in A were expressed in bacteria, and the crude lysates were analyzed by SDS–PAGE and transferred to a PVDF membrane. The lower panel is a Ponceau S–stained blot showing the positions (asterisks) and relative amounts of the various fusion proteins. Top, the same blot after probing with purified recombinant RhoA containing an S-Tag epitope, followed by S-protein–conjugated to HRP (RhoA overlay). (C) The C1 domains of DGKζ are necessary for RhoA interaction. Lysates of wild-type MEFs transfected with HA-tagged, wild-type DGKζ (HA-DGKζ^{wt}) or a mutant missing amino acids 97–233 (HA-DGKζ$^{\Delta 97-233}$) were incubated with beads charged with GST alone, GST-RhoA^{V14}, or GST-RhoA^{N19}. Roughly equal amounts of each protein are shown in the Ponceau S blot. Bound proteins were detected by immunoblotting with an anti-HA antibody. (D) The DGKζ C1A domain (amino acids 97–152) binds RhoA, Rac1, and RhoGDI. The indicated GST-DGKζ fusion proteins were probed with purified recombinant S-tagged RhoA, Rac1, or RhoGDI, followed by S-protein–HRP. (E) Rescue of RhoA activity requires the DGKζ C1 domains. DGKζ-null fibroblasts were transfected with HA-tagged DGKζ^{wt} or DGKζ$^{\Delta 97-233}$. RhoA activity was measured as in Figure 1A after serum stimulation of the cells. The values below the immunoblots represent the fold enrichment in RhoA activity compared with control untransfected cells. (F, G) DGKζ associates with the C-terminal region of RhoA. Lysates from MEFs expressing HA-tagged, wild-type DGKζ were incubated with approximately equal amounts of the indicated GST-fusion proteins. Bound proteins were detected by immunoblotting with an anti-HA antibody. Input represents 10% of the total lysate.

stress fibers in null cells, we assessed whether exogenous expression of HA-tagged DGKζ could restore normal stress fibers. Null cells expressing wild-type (wt) or kinase-dead (kd) DGKζ had significantly fewer condensed F-actin structures than uninfected null cells (Figure 7B). Of interest, DGKζ-expressing cells also displayed many fine, parallel stress fibers, whereas nonexpressing cells had thicker and sparser actin bundles (Figure 7C). HA-DGKζ-expressing cells (wt or kd) were significantly more likely to have fine stress fibers than uninfected null cells (Figure 7D). Collectively these results suggest reintroduction of DGKζ is sufficient to correct the stress fiber defect of null cells. Furthermore, DGKζ overexpression increased the proportion of cells with fine stress fibers in a manner independent of its kinase activity.

Activation of RhoA signaling downstream of extracellular matrix adhesion also leads to the assembly of FAs at the ends of stress fibers. FA formation in wild-type and null MEFs was assessed by immunostaining for paxillin. In wild-type cells, FAs were found primarily at the cell periphery, as expected (Figure 7A). In contrast, null cells appeared to have more FAs in central regions, which coincided with the ends of stress fibers from condensed F-actin structures. Consistent with this observation, null cells had approximately twofold increase in the area occupied by centrally located adhesions (Figure 7E) and a corresponding decrease in peripheral adhesion area (unpublished data). Quantification of the total cellular area occupied by FAs revealed no significant difference between wild-type and null cells (unpublished data). Exogenous expression of

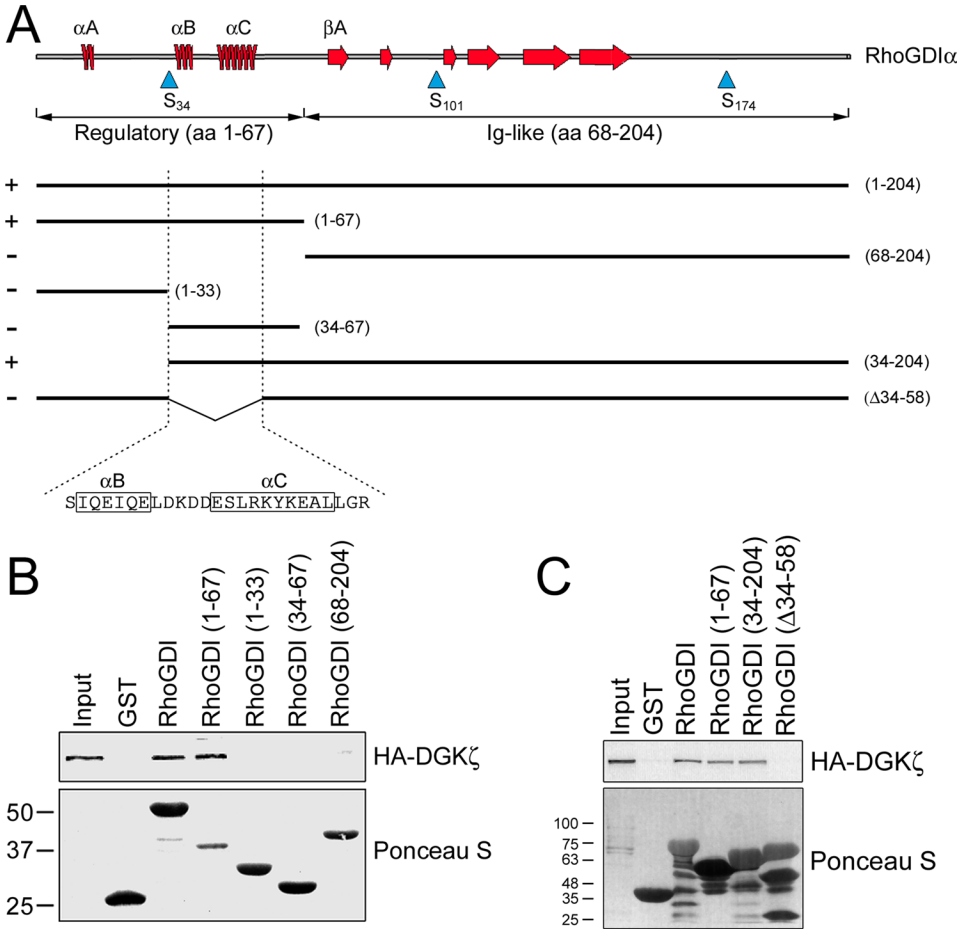

FIGURE 5: A segment of the RhoGDI regulatory domain binds DGKζ. (A) Schematic showing the secondary structure of RhoGDI and selected serine phosphorylation sites (blue triangles). The amino acid boundaries of the regulatory and IgG-like domains are indicated. A plus sign indicates an interaction of the indicated region with DGKζ in pull-down assays; a minus sign indicates no detectable interaction. The amino acid sequence of the putative minimal binding region (residues 34–58) is indicated by the dashed lines. (B, C) Pull-down assays with GST-RhoGDI fusion proteins. MEFs were infected with an adenoviral vector encoding HA-DGKζ, and the lysates were incubated with beads charged with GST alone or with the indicated fusion proteins. Bound proteins were detected by immunoblotting with an anti-HA antibody. Input represents 10% of the extract used for the pull down.

HA-tagged, wild-type or kinase-dead DGKζ restored central FA area to levels comparable with wild-type cells (Figure 7E). These data suggest the reintroduction of DGKζ was sufficient to rescue the aberrant FA localization of null cells and that DGKζ is required for the proper localization and/or turnover of FAs in fibroblasts spreading on fibronectin.

The balance of activity of two RhoA effectors, ROCK and mammalian diaphanous 1 (mDia1), determines the thickness and proper organization of actin stress fibers (Watanabe *et al.*, 1999). The condensed F-actin structures observed in spreading DGKζ-null fibroblasts are reminiscent of the phenotype induced by expression of constitutively active ROCK mutants (Leung *et al.*, 1996; Amano *et al.*, 1997; Ishizaki *et al.*, 1997). To determine whether the condensed F-actin structures in null cells are dependent on ROCK activity, we treated null cells with the ROCK inhibitor Y-27632. Although normal stress fibers were not restored, the condensed F-actin structures were significantly reduced (Figure 8, A and B).

To determine whether signaling downstream of RhoA is affected by the loss of DGKζ, we analyzed the phosphorylation status of two well-known ROCK targets, cofilin and myosin light chain (MLC), under a variety of conditions. ROCK directly phosphorylates MLC (Amano *et al.*, 1996) and prevents its dephosphorylation by inhibiting MLC phosphatase, whereas cofilin is a substrate for LIM kinase, which itself is activated by ROCK-mediated phosphorylation (Amano *et al.*, 2010). Immunoblotting of DGKζ-null fibroblast lysates with phospho-specific antibodies revealed a substantial decrease in phosphorylated cofilin (Ser-3) and phospho-MLC (Ser-19) compared with wild-type fibroblast lysates (Figure 8C). These results suggest there is a decrease in RhoA-mediated activation of ROCK signaling in DGKζ-null cells.

DISCUSSION

Accumulating evidence suggests the selective dissociation of Rho GTPases from RhoGDI involves the phosphorylation of key residues on RhoGDI. For example, PAK1 mediates the selective release of Rac1 by phosphorylating Ser-101 and Ser-174, which lie adjacent to the isoprenyl-binding pocket in the IgG-like domain of RhoGDI (Dermardirossian *et al.*, 2004). The dissociation of RhoA involves PKCα-mediated phosphorylation of Ser-34 in the N-terminal regulatory arm of RhoGDI (Dovas *et al.*, 2010). In another example,

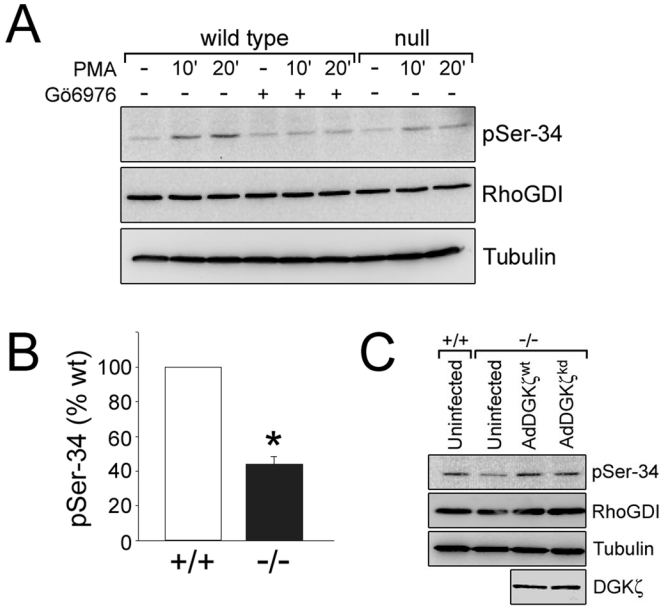

FIGURE 6: Loss of DGKζ impairs PKCα-dependent phosphorylation of RhoGDI on Ser-34. (A) Wild type (+/+) and DGKζ-null (–/–) fibroblasts were treated with vehicle (dimethyl sulfoxide) or 200 nM PMA for 10 or 20 min in the presence or absence of the PKCα/β inhibitor Gö6976. The lysates were immunoblotted with an antibody that specifically recognizes RhoGDI phosphorylated on Ser-34 and with antibodies to RhoGDI and tubulin. (B) Quantification of pSer-34 RhoGDI levels after 20 min of PMA stimulation. The data were normalized to the total amount of RhoGDI in each lane. The pSer-34 level in PMA-stimulated wild-type cells was defined as 100%. Values are the mean ± SEM of three independent experiments. The asterisk indicates a statistically significant difference from wild type ($p < 0.001$) by Student's *t* test. (C) Rescue of RhoGDI Ser-34 phosphorylation activation does not require DGKζ catalytic activity. DGKζ-null cells were infected with adenovirus bearing HA-tagged wild-type ($AdDGK\zeta^{wt}$) or a kinase-dead mutant ($AdDGK\zeta^{kd}$). pSer-34 RhoGDI was assayed as in A after 20 min of PMA stimulation. The levels of RhoGDI, tubulin, and exogenous DGKζ are shown.

fibroblast growth factor 2 binding to S4 activates PKCα, which phosphorylates RhoGDI on Ser-96 and triggers the release of RhoG from a complex containing S4 and the scaffold protein synectin (Elfenbein *et al.*, 2009). Findings such as these have led to the suggestion that phosphorylation of RhoGDI on different residues might function as a type of "release code" (Dermardirossian and Bokoch, 2005), but it remains unclear how such changes differentially affect the dissociation of Rho proteins, since structural studies showed that key residues making contact with RhoGDI are conserved among RhoA, Rac1, and Cdc42 (Longenecker *et al.*, 1999; Hoffman *et al.*, 2000; Scheffzek *et al.*, 2000; Grizot *et al.*, 2001).

Our findings suggest such specificity is imparted by the formation of distinct signaling complexes with RhoGDI. In a previous report, we showed that Rac1 exists in a multiprotein complex with DGKζ, syntrophin, PAK1, and RhoGDI (Abramovici *et al.*, 2009). On PDGF treatment of MEFs, DGKζ stimulates the production of PA, which induces PAK1 activity and subsequently phosphorylates RhoGDI and releases Rac1 for activation. PAK1-mediated phosphorylation of RhoGDI in vivo does not dissociate RhoA/RhoGDI complexes, however, supporting the idea that a distinct mechanism is involved in the release and activation of RhoA (Dermardirossian *et al.*, 2004). In this article, we provide evidence that DGKζ is an integral component of a separate signaling complex that functions as a RhoA-selective RhoGDI dissociation factor.

DGKζ mediates the formation of a PKCα/RhoA/RhoGDI/syntrophin signaling complex

Coimmunoprecipitation experiments suggest DGKζ is required for the efficient interaction of PKCα and RhoA. In DGKζ-null cells there was an ~2.5-fold decrease in the amount of RhoA that coprecipitated with PKCα. These results are consistent with a previous study that showed that PKCα and RhoA functionally interact in vivo and that coexpression of active RhoA and wild-type PKCα enhanced AP-1 transcriptional activity (Chang *et al.*, 1998). However, the authors were unable to detect a direct physical interaction between the two proteins. A later study showed that PKCα interacts directly with RhoA in vitro and results in kinase activation (Slater *et al.*, 2001). These findings, together with data showing that DGKζ binds directly to both proteins (Luo *et al.*, 2003a; Figure 4), suggest there is a weak interaction between PKCα and RhoA that is enhanced by interactions with DGKζ and are consistent with the idea that DGKζ functions as a scaffold to assemble these proteins into a complex. DGKζ was additionally required to mediate the association of syntrophin with RhoA. Collectively these results suggest DGKζ is a core component of a signaling complex containing RhoA, PKCα, RhoGDI, and syntrophin.

DGKζ is required for optimal Ser-34 phosphorylation

Although DGKζ was not required for the interaction of RhoGDI and PKCα, it was necessary for optimal Ser-34 phosphorylation after stimulation with either phorbol ester, which triggers membrane protrusion and increased RhoA levels (Dovas *et al.*, 2010), or serum. Serum contains lysophosphatidic acid (LPA), which activates RhoA downstream of G protein–coupled LPA receptors (Kranenburg and Moolenaar, 2001). However, we cannot rule out possible indirect effects of serum growth factors on Rac1, which could feed back to negatively regulate RhoA activation and Ser-34 phosphorylation. Nevertheless, rescue experiments with exogenous wild-type or kinase-dead DGKζ strongly suggest DGKζ's scaffolding function is requisite for efficient Ser-34 phosphorylation.

Structural studies of RhoGDI in complex with Rho GTPases showed that the otherwise flexible N-terminal regulatory arm makes extensive interactions with the GTPase switch I and II regions, which stabilize the RhoGDI secondary structure (Longenecker *et al.*, 1999; Hoffman *et al.*, 2000; Scheffzek *et al.*, 2000). Several amino acids that make contact with the GTPase lie immediately adjacent to Ser-34. Thus its phosphorylation has been postulated to disrupt key stabilizing interactions to cause RhoA release (Dovas *et al.*, 2010). The binding site for DGKζ resides within an ~25–amino acid region in the RhoGDI regulatory arm that includes Ser-34, the αB and αC helices, and the intervening loop (Figure 5). Thus DGKζ binding to RhoGDI might stabilize the helix-loop-helix secondary structure and position Ser-34 for efficient phosphorylation.

Differential regulation of Rac1 and RhoA activity

PKCα-mediated phosphorylation of RhoGDI on Ser-34 results in a decreased affinity for RhoA but not for Rac1 or Cdc42 (Dovas *et al.*, 2010). The canonical mechanism of PKCα activation involves DAG binding to the C1 domain and Ca^{2+}-dependent binding of phosphatidylserine to the C2 domain (Newton, 2010). Because DGKζ directly interacts with PKCα and inhibits its activity by attenuating the local accumulation of signaling DAG (Luo *et al.*, 2003a), it would be expected to negatively regulate Ser-34 phosphorylation and RhoA activation if the canonical mechanism of PKCα activation was

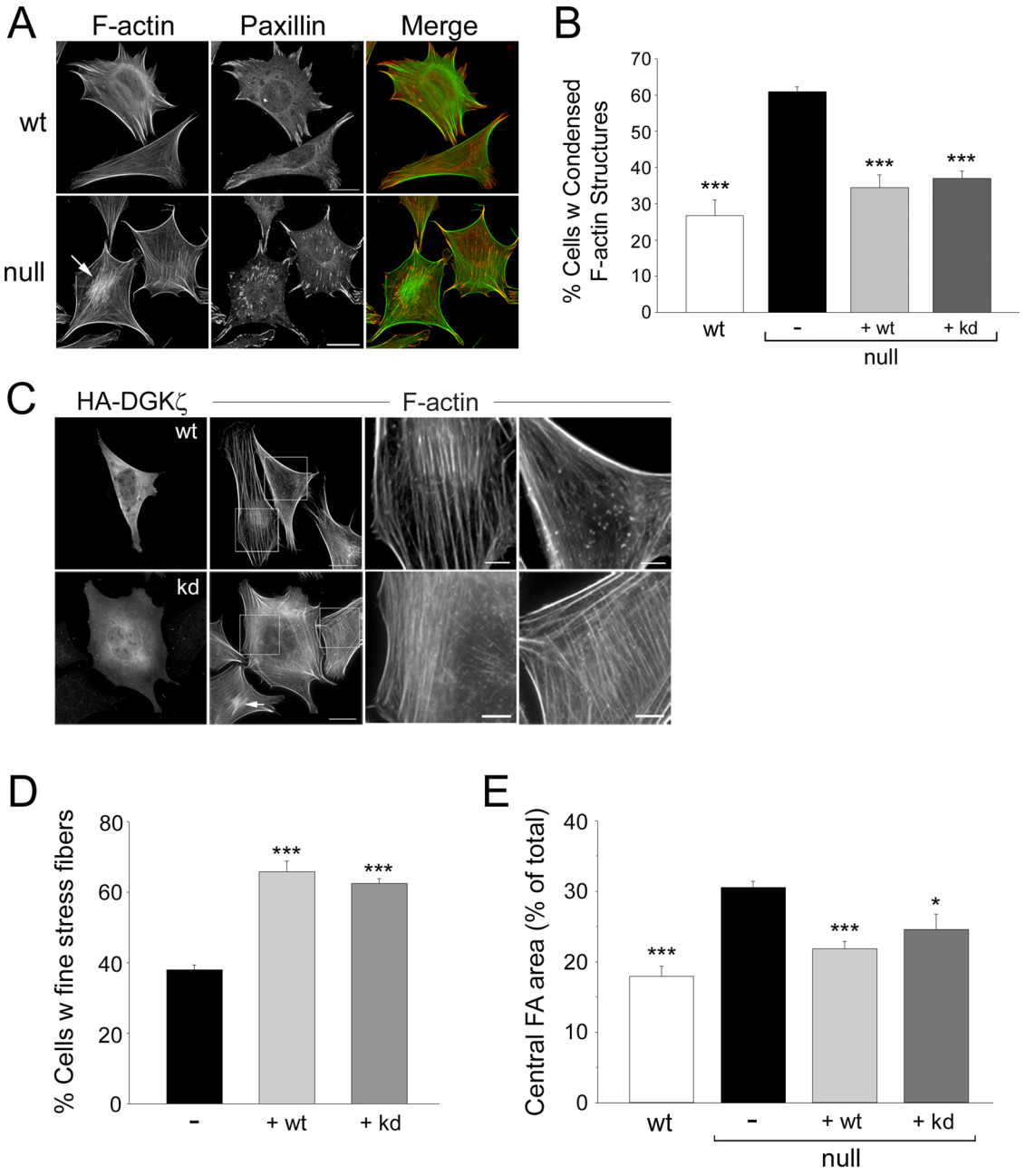

FIGURE 7: Impaired stress fiber and focal adhesion formation in DGKζ-null fibroblasts. (A) Representative images of wild-type (wt) and DGKζ-null (null) fibroblasts taken 120 min after replating on fibronectin. The cells were fixed and labeled with Alexa Fluor 488–conjugated phalloidin (green) to visualize F-actin and immunostained for paxillin, followed by Alexa Fluor 594–conjugated secondary antibody (red), to visualize FAs. The arrow indicates a condensed F-actin structure in a null cell. Scale bars, 20 um (B) Graph showing the percentage of wild-type and DGKζ-null cells with condensed F-actin structures. Null cells were uninfected (–) or infected with HA-tagged, wild-type (+ wt) or kinase-dead (+ kd) DGKζ. Values are the mean ± SEM from three independent experiments. (C) Representative images of DGKζ-null cells infected with wild-type (wt) or kinase-dead (kd) HA-DGKζ. The cells were fixed and stained with anti-HA, followed by Alexa Fluor 594–conjugated secondary antibody to visualize DGKζ and with Alexa Fluor 488–conjugated phalloidin to visualize F-actin. Magnified images of the boxed regions are shown at the right. The arrow indicates a condensed F-actin structure in a null cell. Scale bars, 20 μm; 5 μm for magnified images. (D) Quantification of fine stress fibers in uninfected null cells or null cells expressing wt or kd DGKζ. Values are the mean ± SEM from at least two independent experiments. (E) Graph showing central FA area as a percentage of total FA area in wild-type cells, uninfected null cells, or null cells infected with wt or kd DGKζ. The area occupied by central FAs was quantified in paxillin-stained cells as described in *Materials and Methods*. Values are the mean ± SEM from three independent experiments. All statistical analyses were performed by a one-way analysis of variance, followed by a Holm–Sidak post hoc multiple-comparison test. Asterisks denote a significant difference from uninfected null cells. *$p < 0.05$, ***$p < 0.001$.

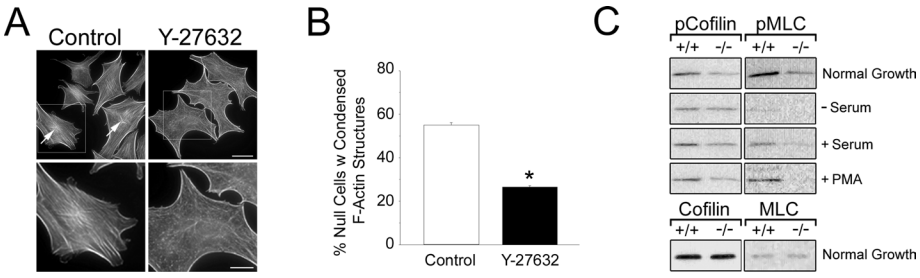

FIGURE 8: Impaired RhoA signaling in DGKζ-null cells. (A) Condensed F-actin structures are dependent on ROCK activity. Representative images of untreated null cells (left) and null cells treated with the ROCK inhibitor Y-27632 (right). The arrows indicate condensed F-actin structures in null cells. Bottom, magnified images of the boxed regions at the top. (B) Graph showing the quantification of condensed F-actin structures in control and Y-27632–treated null cells. Values are the mean ± SEM of three replicates from one experiment and are representative of two independent experiments. At least 300 cells were counted per condition. (C) Approximately equal amounts of lysate from wild-type (+/+) and DGKζ-null (–/–) MEFs grown under different conditions (growth, serum starved, serum stimulated, and PMA stimulated) were immunoblotted with antibodies to pSer-3 of cofilin and pSer-19 of myosin light chain (pMLC; top) or with antibodies to cofilin and MLC (bottom).

involved. However, efficient Ser-34 phosphorylation was stimulated by phosphatidylinositol 4,5-bisphosphate ($PI(4,5)P_2$)–mediated activation of PKCα rather than by the canonical pathway (Dovas *et al.*, 2010). Therefore the conversion of DAG to PA by DGKζ (i.e., its enzymatic activity) should not affect RhoA activation. This is consistent with the ability of catalytically inactive (kinase dead) DGKζ to rescue RhoA activation, Ser-34 phosphorylation, and the stress fiber/FA defect of DGKζ-null cells. This further supports the idea that DGKζ functions primarily as a scaffold to bring together components of the RhoA activation complex.

The balance between the opposing activities of Rac1 and RhoA is a critical determinant of cellular morphology and migratory behavior. Recent findings suggest there is a complex coordination of the activities of the two GTPases within regions undergoing cytoskeletal rearrangements (Spiering and Hodgson, 2011). For example, studies of leading-edge protrusions in migrating MEFs suggest Rac1 and RhoA operate antagonistically in a manner requiring fine spatial and temporal tuning of their activity (Machacek *et al.*, 2009). Our finding that DGKζ catalytic activity is required for Rac1 activation but not RhoA activation suggests a mechanism to regulate the balance of their activities. Decreased DGKζ catalytic activity would reduce Rac1 activation, leading to a relative increase in RhoA activation. Because Rac1 and RhoA are mutually inhibitory (Rottner *et al.*, 1999; Sander *et al.*, 1999; Arthur and Burridge, 2001; Nimnual *et al.*, 2003; Ohta *et al.*, 2006), this effect would be amplified by decreased inhibition of RhoA by Rac1. One way to decrease DGKζ activity is via phosphorylation of Ser-265 in the myristoylated alanine-rich C-kinase substrate (MARCKS) domain by PKCα, which causes an approximately twofold reduction in kinase activity (Luo *et al.*, 2003b). Thus PKCα-mediated phosphorylation of the DGKζ MARCKS domain might serve as a switch, which, when activated, would lead to decreased Rac1 signaling and increased RhoA signaling.

Altered stress fiber and focal adhesion formation in DGKζ-null cells

DGKζ-null cells exhibit conspicuous changes in stress fiber organization while spreading on fibronectin substrates, most notably the formation of condensed F-actin structures (also known as centrally radiating actin bundles). These atypical stress fibers often terminated in the central region of the cell and thus engendered a change in the distribution of FAs—decreased peripheral FAs and a corresponding increase centrally. These findings suggest a defect in FA formation or turnover. Consistent with the latter, phosphorylated PAK1, which is known to promote FA disassembly (Manser *et al.*, 1997), fails to associate with FAs in DGKζ-null cells (Abramovici *et al.*, 2009). Of interest, inhibition of PAK activity was shown recently to increase the distribution of FAs throughout the ventral surface of PtK1 kidney epithelial cells. This was attributed to impaired rates of FA assembly and disassembly, resulting in greatly increased FA lifetime (Delorme-Walker *et al.*, 2011). Thus the absence of PAK activity at FAs in DGKζ-null cells may prolong FA duration, resulting in their altered subcellular distribution. In any case, our findings, taken together, suggest the absence of DGKζ results in decreased RhoA activation, which alters stress fiber formation and FA localization.

Aberrant signaling downstream of RhoA in DGKζ-null cells

In cells spreading on adhesive substrates, the balance of activity of two RhoA effectors, ROCK and mDia1, determines the thickness and proper organization of actin stress fibers (Watanabe *et al.*, 1999), but the relative contributions of each pathway to stress fiber formation have not been established quantitatively. The condensed F-actin structures and centrally located FAs observed in spreading DGKζ-null MEFs are reminiscent of the phenotype induced by expression of constitutively active ROCK mutants (Leung *et al.*, 1996; Amano *et al.*, 1997; Ishizaki *et al.*, 1997). Coexpression of active mutants of mDia1 corrected the phenotype and produced well-aligned stress fibers and normally distributed FAs (Watanabe *et al.*, 1999). Therefore one possible explanation for the abnormal stress fibers and peripheral FAs in DGKζ-null fibroblasts is an increase in ROCK activity relative to mDia1. Consistent with this idea, treatment of null cells with the ROCK inhibitor Y-27632 significantly reduced the percentage of cells with condensed F-actin structures. Moreover, rescue of null cells by DGKζ overexpression gave rise to many thin, parallel stress fibers, indicative of increased mDia1 signaling (Watanabe *et al.*, 1999). However, we documented a decrease in phosphorylation of two key ROCK targets in null cell lysates, consistent with reduced ROCK activity relative to wild-type cells. Decreased RhoA activity in DGKζ-null cells might be expected to lead to an equivalent reduction in mDia1 activity, but a direct measurement of its activity is lacking. Even with a suitable measure, one could not conclude with certainty the relative influence of each effector on stress fiber formation. Furthermore, reduced Rac1 activity in DGKζ-null cells (Abramovici *et al.*, 2009) and the extensive cross-talk between the Rac1 and RhoA signaling pathways (Huveneers and Danen, 2009; Pertz, 2010) make it difficult to predict the net effect on actin regulation. Thus additional experiments are required to precisely map the downstream consequences of reduced RhoA function in DGKζ-null cells. Nevertheless, our results show that the absence of DGKζ perturbs RhoA-mediated stress fiber formation and FA distribution in fibroblasts, possibly by altering the balance of downstream RhoA signaling pathways.

Conclusions

Collectively our findings presented here and elsewhere (Abramovici *et al.*, 2009; Dovas *et al.*, 2010) suggest DGKζ is central to the

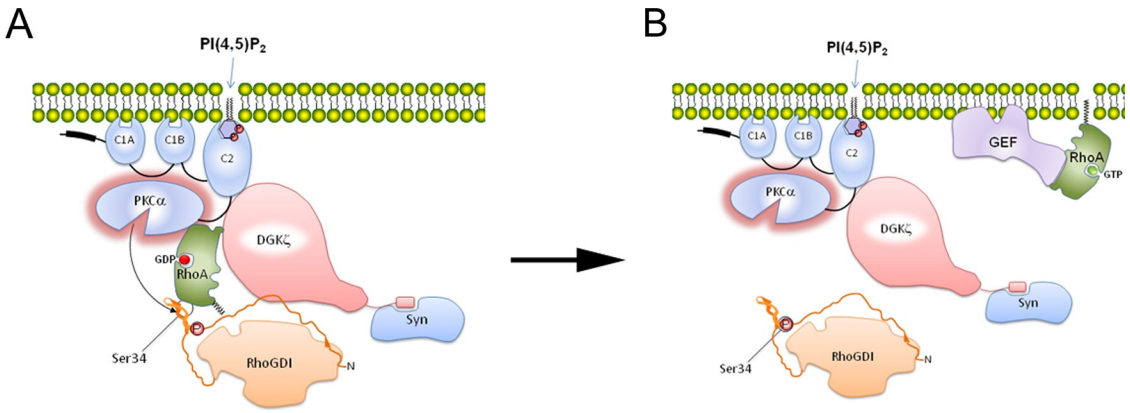

FIGURE 9: Model of RhoA activation in a DGKζ-dependent signaling complex. (A) DGKζ directly interacts with PKCα, RhoA, RhoGDI, and syntrophin to assemble a signaling complex that functions as a RhoA-selective RhoGDI dissociation factor. PI(4,5)P_2 activation of PKCα induces phosphorylation of Ser-34 of RhoGDI. (B) Phosphorylated RhoGDI dissociates from RhoA, allowing its subsequent membrane localization and activation by GEFs.

activation of both Rac1 and RhoA. In the former case, DGKζ generates a product (PA) that stimulates PAK1 activity, phosphorylation of RhoGDI on Ser-101 and Ser-174, and Rac1 dissociation. In the latter, its enzymatic activity is dispensable. Instead, DGKζ provides a scaffold for the assembly of a distinct, multiprotein signaling complex that functions as a GDI dissociation factor specific for RhoA: PKCα activated by PI(4,5)P_2 phosphorylates RhoGDI on Ser-34 and releases RhoA (Figure 9). As a regulator of Rac1 and RhoA activity, DGKζ is positioned at a critical point linking changes in lipid signaling molecules to actin reorganization. Disrupting DGKζ function may affect the balance of Rac1 and RhoA activity, with adverse consequences on downstream signaling and aberrant changes to the actin cytoskeleton.

MATERIALS AND METHODS

Antibodies

An affinity-purified polyclonal antibody raised against the N-terminus of DGKζ has been described previously (Topham *et al.*, 1998). Monoclonal and polyclonal anti-HA and monoclonal anti-tubulin antibodies were purchased from Sigma-Aldrich (St. Louis, MO). Antibodies to RhoA and RhoGDI were obtained from Santa Cruz Biotechnology (Santa Cruz, CA). Rabbit polyclonal antibodies against cofilin, phospho-cofilin (Ser 3), myosin light chain (MLC), and phospho-MLC (Ser-19) were from Cell Signaling Technology (Boston, MA). Mouse anti-paxillin was from BD Biosciences (Franklin Lakes, NJ). Monoclonal His_6 antibody was from Abcam (Cambridge, MA), and monoclonal anti–c-myc antibody was from Roche Applied Science (Indianapolis, IN). Alexa Fluor 488– and 594–conjugated secondary antibodies and phalloidin were purchased from Invitrogen (Carlsbad, CA). HRP-conjugated anti-rabbit and anti-mouse secondary antibodies were from Jackson ImmunoResearch Laboratories (West Grove, PA).

Plasmids

The Rhotekin-RBD construct was described previously (Ren *et al.*, 1999). Plasmids encoding wild-type DGKζ and a kinase-dead mutant (DGKζ^{kd}), both with three tandem, N-terminal HA epitope tags, were as described (Topham *et al.*, 1998; Hogan *et al.*, 2001). A plasmid encoding N-terminal, myc-tagged wild-type RhoA in pEFm-PLINK was a gift from Andrew Thorburn, University of Colorado, Denver. N-terminal (2X) myc-tagged versions of RhoA^{G14V} and RhoA^{T19N} in pcDNA3.1(+) were obtained from the Missouri S&T cDNA Resource Center (www.cdna.org). The inserts were each excised with *Not*I and *Eco*RI restriction enzymes and shuttled into pcDNA3.1(+) with a different multiple cloning site. Then the inserts were excised with *Eco*RI and *Xho*I and subcloned into pGEX-4T-3. For overlay assays, wild-type RhoA and Rac1^{V12} were subcloned into the *Bam*HI and *Eco*RI sites of the pET-32a expression vector. RhoGDI was subcloned into the *Eco*RI and *Xho*I sites.

Cell culture, transfection, and adenoviral infection

Immortalized MEF cell lines have been described previously (Abramovici *et al.*, 2009). MEFs were cultured in DMEM supplemented with 10% fetal calf serum, 2 mM L-glutamine, 100 U/ml penicillin, and 100 U/ml streptomycin and were grown at 37°C in 5% CO_2.

MEFs were transfected using FuGENE 6 (Roche, Indianapolis, IN) according to manufacturer's instructions. The cloning and production of adenoviral constructs have been described previously (Yakubchyk *et al.*, 2005). For adenoviral overexpression experiments, fibroblasts were infected at a multiplicity of infection of 100 for 1 h at 37°C. Cells were incubated for an additional 24–36 h under standard growth conditions.

Cell-spreading assays

Cell-spreading assays were performed essentially as described (Wagner *et al.*, 2002). Briefly, serum-starved cells were washed in phosphate-buffered saline (PBS), pH 7.4, and then harvested with 2 ml of trypsin-EDTA solution. Trypsin was inactivated with 2 ml of a 1-mg/ml soybean trypsin inhibitor solution. Cells were collected by centrifugation and washed three times with warmed 1% bovine serum albumin (BSA) in DMEM (filtered). Finally, the cells were resuspended in 5 ml of the same solution and held in suspension at 37°C for 1 h. The cells were replated at a density of 2×10^4 on fibronectin-coated coverslips for indicated times and then fixed and prepared for immunofluorescence microscopy. For ROCK inhibition experiments, DGKζ-null cells were incubated 60 min before and throughout the spreading assay with 10 μM Y-27632.

Immunofluorescence microscopy

Briefly, cells were rinsed with PBS, pH 7.4, and fixed in 4% paraformaldehyde for 15 min. After permeabilization with 0.5% Triton X-100 in PBS for 10 min, the cells were incubated in blocking buffer (1% BSA in PBS; filtered) for 30 min at room temperature. F-actin was stained using Alexa Fluor 488–conjugated phalloidin, and FAs were

visualized using a paxillin-specific monoclonal antibody, followed by goat anti-mouse Alexa Fluor 594–conjugated secondary antibody.

Quantification of focal adhesion area in spreading cells

Digital images were obtained using Zeiss AxioVision software, version 4.8.2.0, and an AxioCam digital camera mounted on a Zeiss AxioSkop2 MOT microscope (Carl Zeiss, Jena, Germany). Quantification of FAs was performed using ImageJ, version 1.44p (National Institutes of Health, Bethesda, MD). A conversion factor was applied to each image to correct the scale. To correct for possible differences in the size of wild-type and DGKζ-null cells, the total area of each cell was calculated from images stained for F-actin. The threshold and wand tools were used to highlight and select each cell, and the "measure" command was applied. Because there was no significant difference in the area of wild-type and null cells, normalization of FA area to cell size was not required. FA area was calculated from images of paxillin immunofluorescence. Cells to be analyzed were isolated using the freehand selection tool, and the area outside the selection was cleared. Background was subtracted using the two-dimensional rolling ball method (radius, seven pixels), and threshold values were adjusted to highlight FAs. The "create selection" command was use to select the FAs, and the area was calculated using the "measure" command. To calculate the FA area within the central region of each cell, the freehand selection tool was used to exclude lamellipodia and filopodia, and the area outside the selection was cleared. Peripheral FA area was the difference between total and central measurements. Threshold values were set to the same as those used previously to calculate the total FA area.

RhoA and Rac1 activity assays

Active RhoA levels were measured using a GST-RBD pull-down assay (Ren *et al.*, 1999). Cells were serum starved overnight and then stimulated with serum for 3 min. The medium was quickly removed, and the cells were immediately harvested in chilled lysis buffer (50 mM Tris-HCl, pH 7.4, 150 mM NaCl, 1% Triton X-100, 50 mM $MgCl_2$, and protease inhibitors). Lysates were centrifuged at 18,000 × *g* for 5 min at 4°C. Equivalent amounts of protein were incubated with GST-RBD beads for 30 min at 4°C. The beads were collected and washed with lysis buffer and boiled in reducing SDS–PAGE sample buffer (RSB). The eluted proteins were assayed for bound RhoA by immunoblotting. For rescue experiments, DGKζ-null MEFs were infected with adenovirus constructs harboring wild-type DGKζ (DGKζ^{wt}) or a kinase-dead mutant (DGKζ^{kd}) as described earlier and grown for an additional 24 h.

Active Rac1 levels were measured using a GST-PBD pull-down assay as described previously (Sander *et al.*, 1998; Abramovici *et al.*, 2009).

Detection of Ser-34 phosphorylation of RhoGDI

The level of Ser-34 phosphorylation of RhoGDI was determined essentially as described previously (Dovas *et al.*, 2010). Briefly, cells were serum starved overnight and stimulated with 800 nM PMA or vehicle (dimethyl sulfoxide) for 10 or 20 min. In some cases, serum-starved cells were stimulated with 20% FBS containing DMEM media for 5 or 10 min or were pretreated with a 1 μM solution of the PKCαβγ-specific inhibitor Gö6976. For rescue experiments, DGKζ-null cells were infected with adenoviral constructs encoding DGKζ as described earlier. Cells were lysed in cold lysis buffer containing protease and phosphatase inhibitors and cleared by centrifugation at 10,000 × *g* for 10 min at 4°C. Equivalent amounts of protein were separated by SDS–PAGE, transferred to polyvinylidene fluoride (PVDF) membranes, and immunoblotted with an affinity-purified antibody against pSer-34 RhoGDI. The pSer-34 levels were normalized to total RhoGDI. The level of tubulin was used as an additional loading control.

Immunoprecipitations

MEFs were harvested in cold lysis buffer, and the resulting extracts were cleared by centrifugation at 10,000 × *g* for 10 min at 4°C. From 1 to 5 μg of antibody was added to 1 mg of protein extract and incubated at 4°C overnight. For coimmunoprecipitation of DGKζ and RhoA from tissue, brains were harvested from 6- to 8-wk-old mice and were homogenized in ice-cold lysis buffer with a Teflon/glass homogenizer. The protein concentration of the lysate was determined by Bradford assay, and 4 mg each of protein was incubated with antibodies against RhoA or IgG for 2 h at 4°C. In all cases, immune complexes were captured using 50 μl of a 50% slurry of protein A/G–Sepharose beads (Santa Cruz Biotechnology). The beads were collected by centrifugation, washed 3 × 5 min each with lysis buffer, and eluted by boiling in RSB. Samples were analyzed by SDS–PAGE and immunoblotting.

Glutathione *S*-transferase pull-down assays

Cells overexpressing HA-tagged, wild-type DGKζ were lysed, and equal amounts of protein were incubated with immobilized GST-fusion proteins for 1 h and washed four times with lysis buffer, and the eluted proteins were assayed for bound proteins by immunoblotting.

Blot overlay assays

The pET-32a expression vector contains sequences encoding thioredoxin, an N-terminal, 15–amino acid S tag, and a His_6 nickel-binding motif. The expressed fusion proteins were recognized by the S-protein–HRP conjugate (Novagen, Gibbstown, NJ) and were purified from the soluble fraction on nickel–Sepharose columns according to the manufacturer's instructions. Blot overlay assays were carried out as essentially as described previously (Gee *et al.*, 2000) with the following modifications. Recombinant RhoA, Rac1, and RhoGDI fusion proteins were purified from bacterial extracts using His-column chromatography. Purified His-fusion proteins were analyzed for purity by Coomassie blue staining following SDS–PAGE, and their concentration was determined by spectrophotometry (A_{280}) and by the Bradford method (Bradford, 1976).

Total bacterial extracts of GST-DGKζ fusion proteins were resolved by SDS–PAGE and transferred to PVDF membranes. Approximately 150 μg each of purified S-tagged fusion protein was diluted in 4 ml of blocking buffer (5% skim milk powder dissolved in 25 mM Tris, pH 7.5, 150 mM NaCl, and 0.1% Tween-20 [TBST]). The resulting solutions were incubated with the membranes for 1–2 h at room temp. The blots were washed three times for 10 min each in TBST, incubated with HRP-conjugated S-protein for 2 h, and finally washed another four times for 10 min in TBST. Bound S-protein–HRP was visualized by enhanced chemiluminescence.

ACKNOWLEDGMENTS

This project was supported by a grant from the Canadian Institutes of Health Research to S.H.G. J.R.C. and A.Y. are supported by the Danish National Research Foundation. A.Y. is additionally supported by the Novo Nordisk Foundation. We are grateful to Helga Agah for expert technical assistance and to Rafael Garcia-Mata and Nafiseh Sabri for critically evaluating the manuscript.

REFERENCES

Abramovici H, Mojtabaie P, Parks RJ, Zhong XP, Koretzky GA, Topham MK, Gee SH (2009). Diacylglycerol kinase zeta regulates actin cytoskeleton reorganization through dissociation of Rac1 from RhoGDI. Mol Biol Cell 20, 2049–2059.

Amano M, Chihara K, Kimura K, Fukata Y, Nakamura N, Matsuura Y, Kaibuchi K (1997). Formation of actin stress fibers and focal adhesions enhanced by Rho-kinase. Science 275, 1308–1311.

Amano M, Ito M, Kimura K, Fukata Y, Chihara K, Nakano T, Matsuura Y, Kaibuchi K (1996). Phosphorylation and activation of myosin by Rho-associated kinase (Rho-kinase). J Biol Chem 271, 20246–20249.

Amano M, Nakayama M, Kaibuchi K (2010). Rho-kinase/ROCK: A key regulator of the cytoskeleton and cell polarity. Cytoskeleton (Hoboken) 67, 545–554.

Arthur WT, Burridge K (2001). RhoA inactivation by p190RhoGAP regulates cell spreading and migration by promoting membrane protrusion and polarity. Mol Biol Cell 12, 2711–2720.

Boulter E, Garcia-Mata R, Guilluy C, Dubash A, Rossi G, Brennwald PJ, Burridge K (2010). Regulation of Rho GTPase crosstalk, degradation and activity by RhoGDI1. Nat Cell Biol 12, 477–483.

Bourne HR, Sanders DA, McCormick F (1990). The GTPase superfamily: a conserved switch for diverse cell functions. Nature 348, 125–132.

Bourne HR, Sanders DA, McCormick F (1991). The GTPase superfamily: conserved structure and molecular mechanism. Nature 349, 117–127.

Bradford MM ((1976). A rapid and sensitive method for the quantitation of microgram quantities of protein utilizing the principle of protein-dye binding. Anal Biochem 72, 248–254.

Chang JH, Pratt JC, Sawasdikosol S, Kapeller R, Burakoff SJ (1998). The small GTP-binding protein Rho potentiates AP-1 transcription in T cells. Mol Cell Biol 18, 4986–4993.

Delorme-Walker VD, Peterson JR, Chernoff J, Waterman CM, Danuser G, Dermardirossian C, Bokoch GM (2011). Pak1 regulates focal adhesion strength, myosin IIA distribution, and actin dynamics to optimize cell migration. J Cell Biol 193, 1289–1303.

Dermardirossian C, Bokoch GM (2005). GDIs: central regulatory molecules in Rho GTPase activation. Trends Cell Biol 15, 356–363.

Dermardirossian C, Schnelzer A, Bokoch GM (2004). Phosphorylation of RhoGDI by Pak1 mediates dissociation of Rac GTPase. Mol Cell 15, 117–127.

Dovas A, Choi Y, Yoneda A, Multhaupt HA, Kwon SH, Kang D, Oh ES, Couchman JR (2010). Serine 34 phosphorylation of rho guanine dissociation inhibitor (RhoGDIalpha) links signaling from conventional protein kinase C to RhoGTPase in cell adhesion. J Biol Chem 285, 23296–23308.

Elfenbein A, Rhodes JM, Meller J, Schwartz MA, Matsuda M, Simons M (2009). Suppression of RhoG activity is mediated by a syndecan 4-synectin-RhoGDI1 complex and is reversed by PKCalpha in a Rac1 activation pathway. J Cell Biol 186, 75–83.

Etienne-Manneville S, Hall A (2002). Rho GTPases in cell biology. Nature 420, 629–635.

Garcia-Mata R, Boulter E, Burridge K (2011). The "invisible hand": regulation of RHO GTPases by RHOGDIs. Nat Rev Mol Cell Biol 12, 493–504.

Gee SH, Quenneville S, Lombardo CR, Chabot J (2000). Single-amino acid substitutions alter the specificity and affinity of PDZ domains for their ligands. Biochemistry 39, 14638–14646.

Grizot S, Faure J, Fieschi F, Vignais PV, Dagher MC, Pebay-Peyroula E (2001). Crystal structure of the Rac1-RhoGDI complex involved in NADPH oxidase activation. Biochemistry 40, 10007–10013.

Hoffman GR, Nassar N, Cerione RA (2000). Structure of the Rho family GTP-binding protein Cdc42 in complex with the multifunctional regulator RhoGDI. Cell 100, 345–356.

Hogan A, Shepherd L, Chabot J, Quenneville S, Prescott SM, Topham MK, Gee SH (2001). Interaction of gamma 1-syntrophin with diacylglycerol kinase-zeta. Regulation of nuclear localization by PDZ interactions. J Biol Chem 276, 26526–26533.

Hurley JH, Newton AC, Parker PJ, Blumberg PM, Nishizuka Y (1997). Taxonomy and function of C1 protein kinase C homology domains. Protein Sci. 6, 477–480.

Huveneers S, Danen EH (2009). Adhesion signaling—crosstalk between integrins, Src and Rho. J Cell Sci 122, 1059–1069.

Ishizaki T, Naito M, Fujisawa K, Maekawa M, Watanabe N, Saito Y, Narumiya S (1997). p160ROCK, a Rho-associated coiled-coil forming protein kinase, works downstream of Rho and induces focal adhesions. FEBS Lett 404, 118–124.

Kranenburg O, Moolenaar WH (2001). Ras-MAP kinase signaling by lysophosphatidic acid and other G protein-coupled receptor agonists. Oncogene 20, 1540–1546.

Leung T, Chen XQ, Manser E, Lim L (1996). The p160 RhoA-binding kinase ROK alpha is a member of a kinase family and is involved in the reorganization of the cytoskeleton. Mol Cell Biol 16, 5313–5327.

Longenecker K *et al.* (1999). How RhoGDI binds Rho. Acta Crystallogr D Biol Crystallogr 55, 1503–1515.

Luo B, Prescott SM, Topham MK (2003a). Association of diacylglycerol kinase ζ with protein kinase Cα: spatial regulation of diacylglycerol signaling. J Cell Biol 160, 929–937.

Luo B, Prescott SM, Topham MK (2003b). Protein kinase Cα phosphorylates and negatively regulates diacylglycerol kinase ζ. J Biol Chem 872, 74593–24593.

Machacek M, Hodgson L, Welch C, Elliott H, Pertz O, Nalbant P, Abell A, Johnson GL, Hahn KM, Danuser G (2009). Coordination of Rho GTPase activities during cell protrusion. Nature 461, 99–103.

Manser E, Huang HY, Loo TH, Chen XQ, Dong JM, Leung T, Lim L (1997). Expression of constitutively active alpha-PAK reveals effects of the kinase on actin and focal complexes. Mol Cell Biol 17, 1129–1143.

Newton AC (2010). Protein kinase C: poised to signal. Am J Physiol Endocrinol Metab 298, E395–E402.

Nimnual AS, Taylor LJ, Bar-Sagi D (2003). Redox-dependent downregulation of Rho by Rac. Nat Cell Biol 5, 236–241.

Nobes CD, Hall A (1995). Rho, rac and cdc42 GTPases: regulators of actin structures, cell adhesion and motility. Biochem Soc Trans 23, 456–459.

Ohta Y, Hartwig JH, Stossel TP (2006). FilGAP, a Rho- and ROCK-regulated GAP for Rac binds filamin A to control actin remodelling. Nat Cell Biol 8, 803–814.

Paterson HF, Self AJ, Garrett MD, Just I, Aktories K, Hall A (1990). Microinjection of recombinant p21rho induces rapid changes in cell morphology. J Cell Biol 111, 1001–1007.

Pertz O ((2010). Spatio-temporal Rho GTPase signaling—where are we now? J Cell Sci 123, 1841–1850.

Ren XD, Kiosses WB, Schwartz MA (1999). Regulation of the small GTP-binding protein Rho by cell adhesion and the cytoskeleton. EMBO J 18, 578–585.

Ridley AJ, Paterson HF, Johnston CL, Diekmann D, Hall A (1992). The small GTP-binding protein rac regulates growth factor-induced membrane ruffling. Cell 70, 401–410.

Rottner K, Hall A, Small JV (1999). Interplay between Rac and Rho in the control of substrate contact dynamics. Curr Biol 9, 640–648.

Sander EE, ten Klooster JP, van Delft S, van der Kammen RA, Collard JG (1999). Rac downregulates Rho activity: reciprocal balance between both GTPases determines cellular morphology and migratory behavior. J Cell Biol 147, 1009–1022.

Sander EE, van Delft S, ten Klooster JP, Reid T, van der Kammen RA, Michiels F, Collard JG (1998). Matrix-dependent Tiam1/Rac signaling in epithelial cells promotes either cell-cell adhesion or cell migration and is regulated by phosphatidylinositol 3-kinase. J Cell Biol 143, 1385–1398.

Scheffzek K, Stephan I, Jensen ON, Illenberger D, Gierschik P (2000). The Rac-RhoGDI complex and the structural basis for the regulation of Rho proteins by RhoGDI. Nat Struct Biol 7, 122–126.

Slater SJ, Seiz JL, Stagliano BA, Stubbs CD (2001). Interaction of protein kinase C isozymes with Rho GTPases. Biochemistry 40, 4437–4445.

Spiering D, Hodgson L (2011). Dynamics of the Rho-family small GTPases in actin regulation and motility. Cell Adh Migr 5, 170–180.

Topham MK, Bunting M, Zimmerman GA, McIntyre TM, Blackshear PJ, Prescott SM (1998). Protein kinase C regulates the nuclear localization of diacylglycerol kinase-zeta. Nature 394, 697–700.

Wagner S, Flood TA, O'Reilly P, Hume K, Sabourin LA (2002). Association of the Ste20-like kinase (SLK) with the microtubule. Role in Rac1-mediated regulation of actin dynamics during cell adhesion and spreading. J Biol Chem 277, 37685–37692.

Watanabe N, Kato T, Fujita A, Ishizaki T, Narumiya S (1999). Cooperation between mDia1 and ROCK in Rho-induced actin reorganization. Nat Cell Biol 1, 136–143.

Yakubchyk Y, Abramovici H, Maillet JC, Daher E, Obagi C, Parks RJ, Topham MK, Gee SH (2005). Regulation of neurite outgrowth in N1E-115 cells through PDZ-mediated recruitment of diacylglycerol kinase kinase ζ. Mol Cell Biol 25, 7289–7302.